Nanoparticle-Guided Biomolecule Delivery for Transgene Expression and Gene Silencing in Mature Plants

Gozde S. Demirer[1], Roger Chang[1], Huan Zhang[1], Linda Chio[1] and Markita P. Landry[1,2,3]*

[1] Department of Chemical Engineering, University of California, Berkeley, CA 94720, USA.
[2] California Institute for Quantitative Biosciences, QB3, University of California, Berkeley, CA 94720, USA.
[3] Chan-Zuckerberg Biohub, San Francisco, CA 94158, USA. *e-mail: landry@berkeley.edu

Genetic engineering of plants is at the core of environmental sustainability efforts, natural product synthesis of pharmaceuticals, and agricultural crop engineering to meet the needs of a growing population changing global climate. The physical barrier presented by the cell wall has limited the ease and throughput with which exogenous biomolecules can be delivered to plants. Current techniques suffer from host range limitations, low transformation efficiencies, toxicity, and unavoidable DNA integration into the host genome. Herein, we demonstrate efficient diffusion-based plasmid DNA and small interfering RNA (siRNA) delivery into two species of mature plants with a suite of pristine and chemically-functionalized high aspect ratio nanomaterials. Efficient DNA delivery and strong transient protein expression is accomplished in mature *Eruca sativa* (arugula) leaves with covalently-functionalized or pristine single-walled and multi-walled carbon nanotubes, with efficiencies comparable to agrobacterium. We also demonstrate nanotube-based transient protein expression in cell wall-free arugula protoplasts with 85% transformation efficiency. Lastly, we demonstrate a second nanoparticle-based strategy in which siRNA is delivered and activated in the *Nicotiana benthamiana* plant cell cytosol, effectively silencing a gene with 95% efficiency. Our work provides a promising tool for species-independent, targeted, and passive delivery of genetic material, without transgene integration, into plant cells for rapid and parallelizable testing of plant genotype-phenotype relationships.

Introduction

Plant bioengineering is critical to address the world's leading challenges in meeting our growing food and energy demands, and as a tool for scalable pharmaceutical manufacturing. Over the past several decades, remarkable progress has been made in bioengineering with the improvement of genome sequencing and editing technologies. Due to these recent advancements, plant synthetic biology and engineering now has tremendous potential to benefit many fields. In agriculture, genetic enhancement of plants can be employed to create crops that are resistant to herbicides[1], insects[2], diseases[3], and drought.[4] In pharmaceuticals and therapeutics, genetically engineered plants can be used to synthesize valuable small-molecule drugs and recombinant proteins.[5] Furthermore, bioengineered plants may provide cleaner and more efficient biofuels.[6,7]

Despite several decades of technological advancements in bioengineering, most plant species remain difficult to genetically transform.[8] The major and inherent challenge facing efficient plant genetic transformation is biomolecule delivery into plant cells through the rigid and multi-layered cell wall. Currently, few delivery tools exist that can transfer biomolecules into plant cells, each with considerable limitations. Agrobacterium-mediated delivery[9] is the most commonly used tool for gene delivery into plants with the limitations of efficient delivery to only a narrow range of plant species, unsuitability for high-throughput applications, and foreign DNA integration into the host genome.[10] The one other commonly used tool for plant transformation is biolistic particle delivery[11] (also called gene gun or particle bombardment), which can deliver DNA into a wider range of plant species but faces limitations of low-level expression of the delivered genes, potential toxicity of the particles used[12], plant cell damage from high bombardment pressures, and random DNA integration into the host genome.[8] Therefore, for plant engineering to reach its full potential, conventional gene delivery methods are due for significant modernization commensurate with advances in molecular bioengineering to address aforementioned limitations.

Nanomaterials are optimal candidates to eliminate current limitations of delivering biomolecules into plants. While nanomaterials have been studied for gene delivery into animal cells[13,14], their potential for plant systems remains under-studied.[15] Under certain nanoparticle surface chemistries, high aspect ratio nanomaterials such as carbon nanotubes (CNTs) have recently been shown to traverse extracted chloroplast[16] and plant[17] membranes owing to several figures of merit: high aspect ratio, exceptional tensile strength, high surface area-to-volume ratio, and biocompatibility with facile surface modification. When bound to CNTs, biomolecules are

protected from cellular metabolism and degradation[18], exhibiting superior biostability compared to free biomolecules. Moreover, single-walled carbon nanotubes (SWCNTs) have strong intrinsic near-infrared fluorescence[19,20] within the tissue-transparency window and thus benefit from reduced imaging autofluorescence, allowing for tracking of SWCNT nanoparticle distribution deep in plant tissues. However, previous incorporation of CNTs in plant systems is limited to exploratory studies of CNT biocompatibility in plants[16,21,22] and sensing of small molecules in plant tissues[17,23] by introducing CNTs complexed to fluorescent dyes or polymers with no biological function.

Herein, we develop and optimize a nanomaterial-based delivery tool that can transfer functional biomolecules into both model and crop plant species with high efficiency. For the first time, we demonstrate efficient transient gene expression and silencing in mature plants through CNT-mediated delivery of functional biomolecules. This platform can enable high-throughput genetic plant transformations for a wide variety of plant genome engineering applications.

Grafting DNA on carbon nanotube scaffolds

In this work, expression of a functional gene is accomplished by delivering plasmids and linear DNA fragments into the mature plant cell nucleus with CNTs. Separately, alternate grafting chemistries enable gene silencing in mature plants, achieved by delivering siRNA into the plant cell cytoplasm with CNT-based nanocarriers (Fig. 1a). For the gene expression study, green fluorescent protein (GFP)-encoding plasmids or their linear fragments (see Methods) are grafted on SWCNTs and multi-walled carbon nanotubes (MWCNTs) through two distinct grafting methods. The first DNA-grafting method involves direct adsorption of DNA on CNTs via dialysis (see Methods). Initially, CNTs are coated with a surfactant – sodium dodecyl sulfate (SDS). During dialysis, SDS desorbs from the CNT surface and exits the dialysis membrane, while DNA adsorbs onto the surface of CNTs in a dynamic ligand exchange process (Fig. 1b). In this method, double-stranded DNA vectors, supplied in excess, graft on CNTs through π-π stacking interactions. The adsorption of DNA on CNTs is confirmed through a wavelength shift in the SWCNT near-infrared fluorescence emission spectra, characteristic of a DNA adsorption-induced change in the CNT dielectric environment[24] (Supplementary Fig. 1). Control dialysis aliquots of SDS coated CNTs in the absence of DNA show rapid CNT precipitation and lack near-infrared fluorescence (Supplementary Fig. 1), confirming DNA adsorption and SDS desorption in our DNA sample. Stable adsorption of DNA on CNTs is separately confirmed via 1% agarose gel electrophoresis (Supplementary Fig. 1).

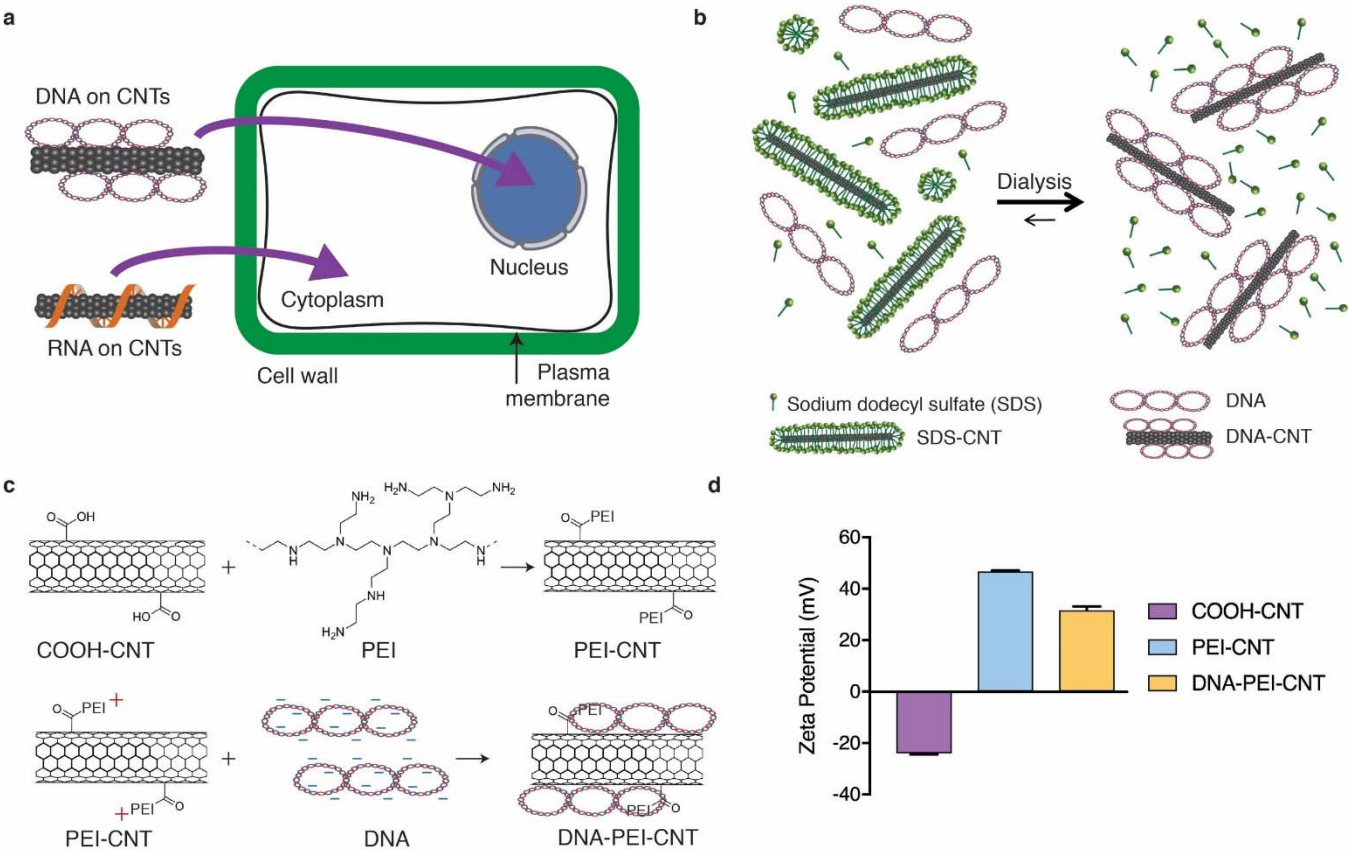

Figure 1. Overarching strategy for CNT-mediated plant transformations and DNA grafting on CNTs. a, For expression of a functional gene, DNA is delivered into the mature plant cell nucleus with carbon nanotubes. Separately, for silencing of a functional gene, siRNA is delivered into the plant cell cytoplasm with carbon nanotubes. **b**, DNA is grafted on CNTs through π-π stacking, in which the initial SDS coating is gradually replaced by DNA adsorption via dialysis. **c**, An alternative method of DNA loading onto CNTs is accomplished through electrostatic grafting, in which carboxylated CNTs (COOH-CNT) are first chemically modified via covalent attachment of a cationic PEI polymer, and subsequently incubated with negatively charged DNA. **d**, PEI and DNA binding on CNTs is validated by zeta potential measurements: The -24 mV zeta potential of COOH-CNT increases to +46 mV after reaction with PEI, due to positively charged PEI binding, and subsequently decreases to +31 mV when incubated with negatively charged DNA, confirming DNA adsorption. Error bars are standard deviations (n = 3).

The second method developed for DNA vector grafting on CNTs is electrostatic grafting, in which carboxylated CNTs (COOH-CNT) are first covalently modified with a cationic polymer (poly-ethyleneimine, PEI) to carry a positive charge. Next, positively charged CNTs (PEI-CNT) are incubated with negatively charged DNA vectors (Fig. 1c). The covalent attachment of PEI and adsorption of DNA on CNTs is confirmed through zeta potential measurements (Fig. 1d). The initial zeta potential of -24 mV for COOH-CNT increases to +46 mV after reaction with positively-charged PEI, and subsequently decreases to +31 mV when incubated with negatively charged DNA, confirming DNA adsorption. DNA adsorption through electrostatic grafting to

CNTs is also confirmed with agarose gel electrophoresis (Supplementary Fig. 1). Additionally, AFM imaging of nanoparticles was used to confirm CNT functionalization and DNA adsorption to CNTs. Nanoparticle heights before and after reaction with PEI are measured to be 6.55 ± 0.60 nm and 12.61 ± 0.87 nm for COOH- and PEI-MWCNT, respectively, confirming PEI binding (Supplementary Fig. 2). AFM also reveals that CNT nanoparticle height increases from 12.61 nm to 21 ± 2.19 nm after incubation with DNA vectors, as expected, further confirming DNA grafting on CNTs (Supplementary Fig. 2).

DNA delivery into mature plants with carbon nanotube scaffolds

Functional gene expression studies are implemented with arugula (*Eruca sativa*) to demonstrate the applicability of our platform to transform crop plants in lieu of traditional laboratory plant species. After GFP-encoding DNA-CNT suspensions are prepared through dialysis and electrostatic grafting, the DNA-CNT conjugates are infiltrated into the leaves of mature arugula plants (3-4 weeks old) from the abaxial surface of the leaf lamina with a needleless syringe (Fig. 2a), (see Methods). Post-infiltration, DNA-CNTs traverse the plant cell wall and membrane to enter the cytosol. In the cytosol, we postulate that either the DNA-CNT complex further transports across the nuclear membrane where DNA desorbs from the CNT surface, or DNA desorbs from the CNT surface inside the cytosol and free DNA travels into the nucleus to initiate gene expression (Fig. 2b). Arugula leaves infiltrated with DNA-CNTs are imaged 72 hours post-infiltration with confocal microscopy, and expression of GFP is observed in the mesophyll cells of the leaf lamina (Fig. 2c). No GFP expression is detected when free DNA vectors or PEI-DNA complexes are delivered without CNT carriers (Supplementary Fig. 3). Z-stack analysis of the fluorescence profile of the DNA-CNT treated leaf shows that GFP fluorescence originates from the full thickness of the leaf, confirming that CNT nanocarriers diffuse and penetrate through the full leaf profile by percolating through ~7 layers of plant cells (Fig. 2d). GFP expression induced by CNT-mediated DNA delivery is transient, and the transgene expression disappears 7 days post-infiltration (Fig. 2e), demonstrating that genes delivered into the plant cell nucleus via CNTs do not integrate into the plant nuclear genome, making CNT-mediated transformation highly beneficial for transgene expression without transgene integration.

The efficiency of CNT nanocarrier internalization and GFP expression varies widely for the different nanomaterial formulations we tested. Quantitative fluorescence intensity analysis of confocal images (see Methods) indicates that GFP expression is significantly higher for DNA-

CNTs prepared through electrostatic grafting compared to GFP expression induced by CNT-DNA conjugates prepared via dialysis (Fig. 2f). Our most efficient DNA-CNT formulation is plasmid DNA delivered with PEI-functionalized SWCNT, which is over 6 times more efficient than plasmid DNA adsorbed to pristine MWCNT via dialysis, our least-efficient DNA-CNT formulation. Our results suggest CNT surface chemistry is an important factor for biomolecule delivery into plant cells. The observed results can be explained by different DNA binding strengths to CNT surfaces in the two DNA grafting methods. The predominant DNA-CNT binding interaction in the case of dialysis is π-π stacking. In contrast, electrostatic attraction is the predominant binding interaction for the electrostatic grafting method. We propose that the smaller equilibrium dissociation constant[25] and higher binding energy value for electrostatic attraction compared to π-π stacking interactions[26] increase the stability of the DNA-CNT complex as it traverses the cell wall, plasma membrane, and nuclear envelope, thus increasing the delivery of DNA to the plant cell nucleus (see Supplementary Information). Conversely, lower genetic transformation efficacies of DNA-CNTs prepared via relatively weak π-π stacking interactions are limited by premature DNA desorption from the CNT, prior to internalizing into the cell and/or nucleus.

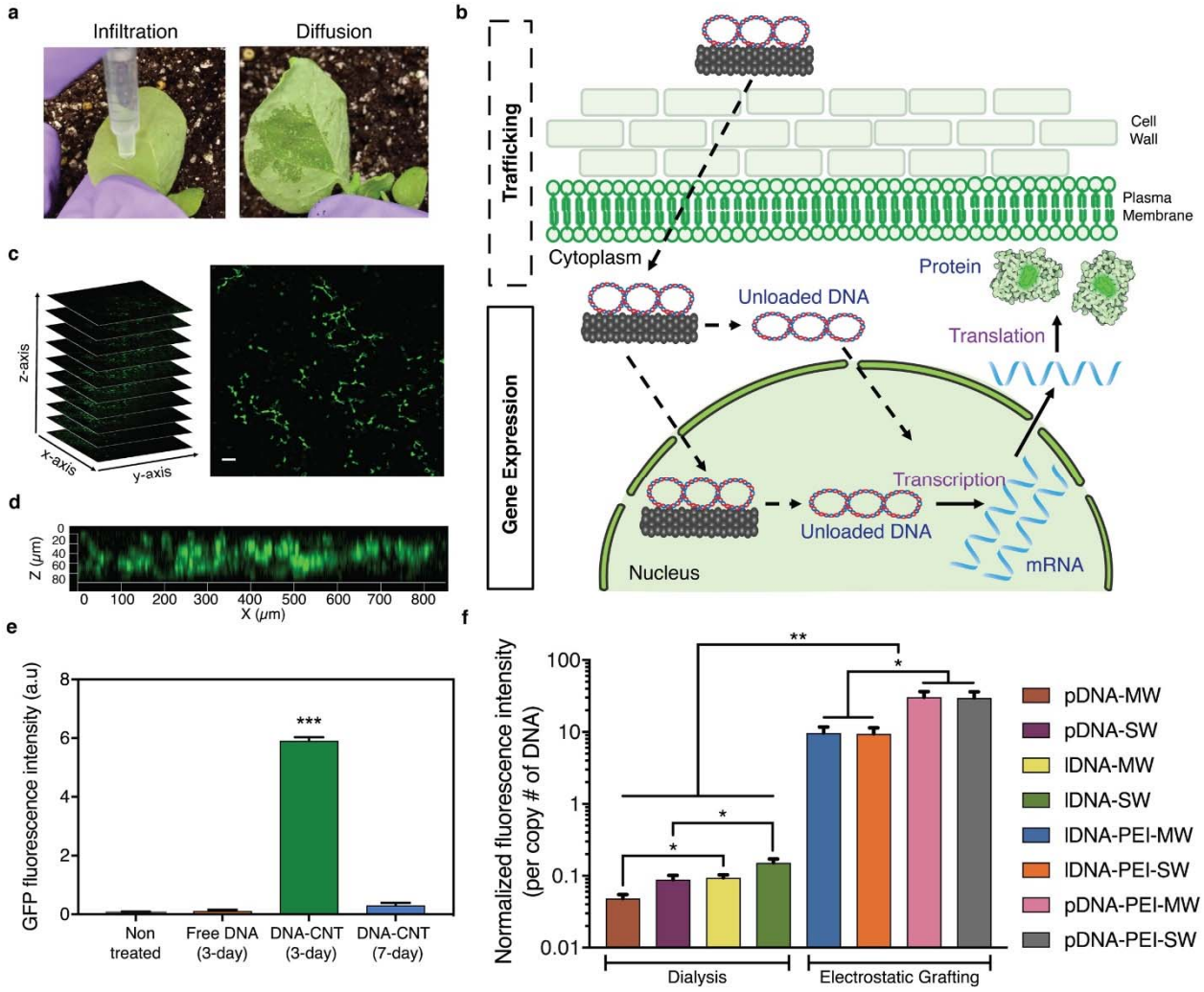

Figure 2. DNA delivery into mature plants with CNTs and subsequent GFP expression. a, DNA-CNT conjugates are infiltrated into the leaves of mature arugula plants from the abaxial surface of the leaf lamina with a needleless syringe **b**, Post-infiltration, DNA-CNTs traverse the plant cell wall and membrane and enter the cytosol where DNA either desorbs in the cytosol and enters the nucleus, or DNA carried by CNTs is transported across the nuclear membrane to initiate gene expression. **c**, Arugula leaves infiltrated with DNA-CNTs are imaged with confocal microscopy, and expression of GFP is observed in the mesophyll cells of the leaf lamina. Scale bar, 50 μm. **d**, Z-stack analysis of the fluorescence profile of the DNA-CNT treated leaf shows that GFP fluorescence originates from the full thickness of the leaf, confirming that CNT nanocarriers diffuse and penetrate through the full leaf profile. **e**, GFP expression induced by CNT-mediated DNA delivery is transient, and the transgene expression has disappeared 7 days post-infiltration. Two-tailed P value for *** is smaller than 0.0001. Error bars are standard errors of the mean (n = 3). **f**, Log-scale graph showing relative GFP expression efficiencies per copy number of DNA. Quantitative fluorescence intensity analysis of confocal images indicates that GFP expression is significantly higher for DNA-CNTs prepared by electrostatic grafting compared to GFP expression induced by DNA-CNT nanocarriers prepared via dialysis. Two-tailed P values for * are smaller than 0.05 and for ** are smaller than 0.01. Error bars are standard errors of the mean (n = 3).

After infiltration into the plant leaves, DNA-CNTs diffuse in the extracellular matrix while simultaneously internalizing into the plant cells. Consequently, there is a point where no nanocarrier is left in the extracellular matrix due to the consumption (internalization) by cells

proximal to the DNA-CNT infiltration area. We analyzed and modeled the spatial distribution of nanocarriers inside the plant leaf with a diffusion-reaction equation in which we implement a first order elementary reaction with a constant rate constant for metabolic consumption of nanocarriers (see Supplementary Information). The model predicts an exponential decay in the concentration of nanocarriers with respect to distance from the infiltration area. To fit this mathematical model to our experimental results, we analyzed the lateral profile of leaf GFP fluorescence expression obtained through confocal imaging as a proxy for nanocarrier diffusivity, and obtained good agreement between our diffusion-reaction model and GFP fluorescence localization (R^2 = 0.996, Supplementary Fig. 4). Additionally, near-infrared fluorescence images of DNA-SWCNT diffusion and lateral spatial distribution in plant leaves matches our observed GFP expression profile (Supplementary Fig. 5).

DNA delivery into isolated protoplasts with carbon nanotube scaffolds

We further investigated the ability of CNT nanocarriers to deliver plasmid DNA and trigger functional gene expression in a different plant system – isolated protoplasts, which are plant cells cultured without cell walls. Currently, protoplasts are used to increase the throughput of plant genetic screens and for synthesis of recombinant proteins, thus needing a facile, passive, high efficiency, and species-independent transformation platform.[27] For this purpose, intact and healthy protoplasts were extracted from arugula leaves through enzymatic cell wall degradation (see Methods, Fig. 3a) with high efficiency and high yield (10^7 total protoplast / 20 leaves). The isolated protoplast solution is subsequently incubated with plasmid DNA-CNTs prepared via dialysis for 24 hours, and subsequently imaged with fluorescence microscopy to gauge GFP expression (see Methods). The GFP-encoding plasmid delivered to protoplasts in these experiments also encodes a nuclear localization signal that transports the expressed GFP protein from the cytosol back into the plant cell nucleus to facilitate imaging and transformation efficiency calculations.[28] Protoplasts incubated with DNA-CNTs show strong GFP expression localized in the nucleus (Fig. 3c), whereas protoplasts incubated with free plasmid DNA without CNT nanocarriers do not show GFP expression (Fig. 3d). Isolated protoplasts transformed with DNA-CNTs show 72% transformation efficiency after a 24-hour incubation period with what we determined to be the optimum DNA concentration of 250 ng/μL (Fig. 3b). Interestingly, high DNA concentrations (~1000 ng/μL) loaded onto the same CNT amount prevent protoplast transformation and adversely affect protoplast health, which may be caused by the highly localized negative charge of concentrated plasmid DNA. Protoplast transformation was also

accomplished by delivering a separate DNA plasmid lacking the nuclear localization signal (see Methods), in which case GFP expression is observed in the protoplast cytosol with 85% transformation efficiency (Supplementary Fig. 6). Our prior work on CNT nanoparticle internalization into extracted plant plastids suggests nanoparticle internalization through the lipid bilayer occurs within seconds of CNT exposure.[16] Thus, our CNT-based plasmid DNA delivery platform enables rapid and passive delivery of DNA into protoplasts and transgene expression with high efficiency and no observable adverse effects to protoplast viability.

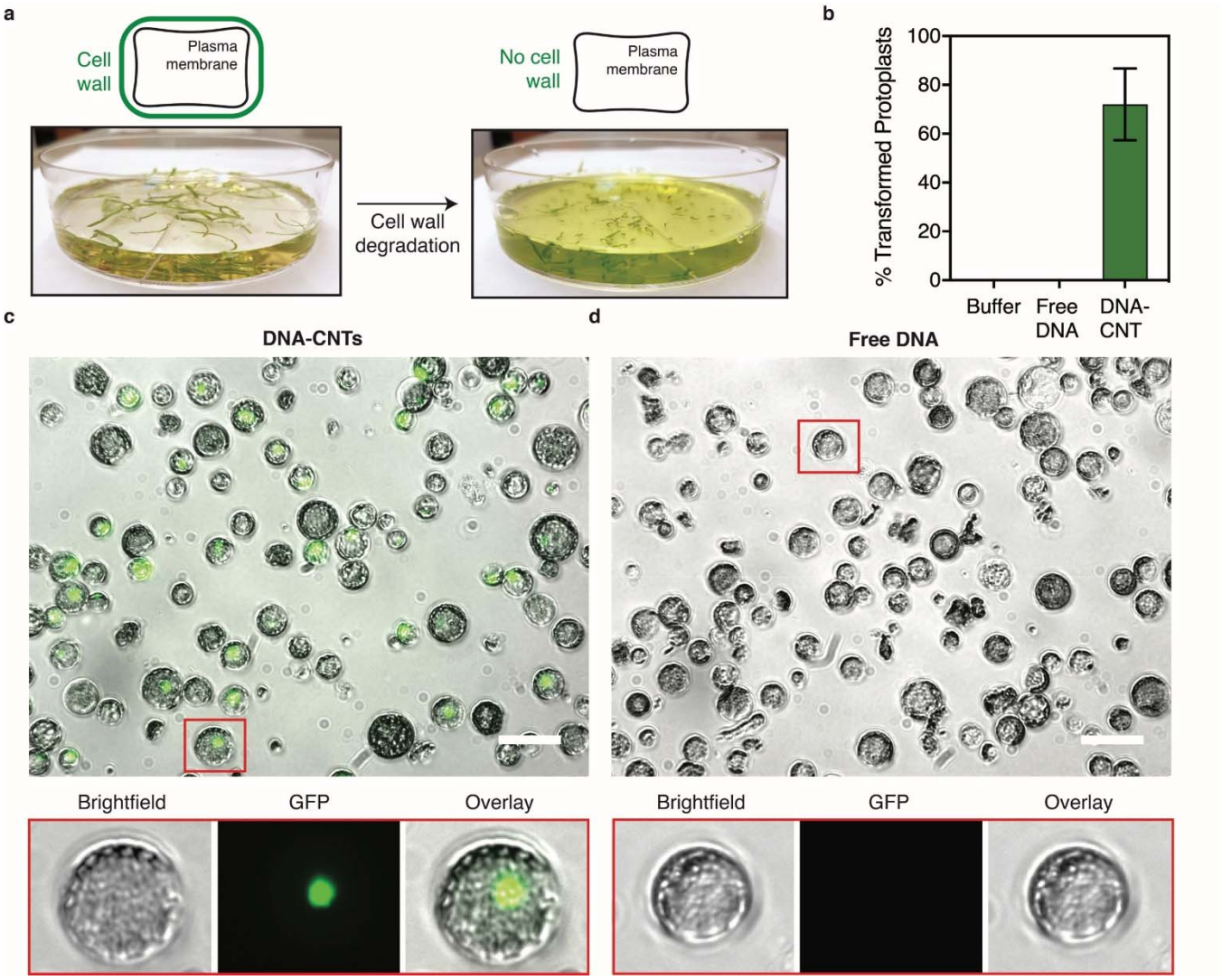

Figure 3. DNA delivery into isolated protoplasts with CNTs and subsequent GFP expression. a, Intact and healthy protoplasts are extracted from arugula leaves through enzymatic cell wall degradation with high efficiency and high yield (10^7 total protoplast / 20 leaves). **b**, Percentage of the total isolated protoplasts transformed with DNA-CNTs is 72% after a 24-hour incubation period with what we determined to be the optimum DNA concentration of 250 ng/μL. Error bars are standard errors of the mean (n = 5). **c**, Protoplasts incubated with DNA-CNTs show strong GFP expression localized in the nucleus. **d**, Protoplasts incubated with free plasmid DNA without CNT nanocarriers do not show GFP expression. Red boxes demonstrate regions of interest that are zoomed in and presented with brightfield, GFP, and overlay channels. Scale bars, 25 μm.

Carbon nanotube-guided siRNA gene silencing in mature plants

We next demonstrate the applicability of our CNT-mediated delivery tool in plants with another broadly-utilized functional cargo – siRNA, which is a short (20-30 bp) single-stranded RNA duplex that acts within the RNA interference pathway for sequence-specific inhibition of gene expression at the mRNA transcript level.[29] As with plasmid DNA, delivery of siRNA has been optimized for most mammalian and bacterial cell culture applications, but remains a significant challenge for mature plants.[30] For this study, we silence a gene in a model transgenic *Nicotiana benthamiana* plant species, which strongly expresses GFP in all cells due to GFP transgene integration in the nuclear genome. To silence this constitutively-expressed GFP gene, we designed a 21-bp siRNA sequence that is specific to the GFP mRNA[31] (Fig. 4a). Loading of siRNA on CNT nanoparticle carriers is accomplished by separate probe-tip sonication of each siRNA single-strand (sense and antisense) of the siRNA duplex with SWCNTs (see Methods), (Fig. 4a). The adsorption of RNA on SWCNTs is confirmed through the emergence of characteristic peaks in the SWCNT near-infrared fluorescence emission spectra for both siRNA sense and antisense suspensions (Supplementary Fig. 7). Equimolar quantities of siRNA sense-CNTs and siRNA antisense-CNTs are mixed immediately prior to infiltration into the leaves of mature mGFP5 *Nicotiana benthamiana* plants (3-4 weeks old) from the abaxial surface of the leaf lamina with a needleless syringe. Post-infiltration, we predict that RNA-CNTs traverse the plant cell wall and membrane, and reach the cytosol. In the plant cell cytosol, the complementary siRNA strands hybridize to each other, desorb from the CNT surface, and induce GFP gene silencing (Fig. 4a). Cytosolic desorption and hybridization claims are supported by our thermodynamic analysis that considers the energetics of hydrogen bonding and π-π stacking interactions which favors siRNA hybridization and desorption over adsorption, only in the intracellular environment (see Supplementary Information and Supplementary Fig. 7).

Nicotiana benthamiana leaves are imaged via confocal microscopy 24-hours after siRNA-CNT infiltration to monitor GFP silencing. Untreated leaves show strong GFP expression, as expected, due to the constitutive expression of GFP in the transgenic plant. Conversely, leaves infiltrated with siRNA-CNTs show strongly reduced GFP fluorescence, suggesting effective siRNA-CNT mediated gene silencing (Fig. 4b and Supplementary Fig. 8). To corroborate our confocal imaging results, we performed quantitative PCR (qPCR) analysis of the siRNA-CNT infiltrated plant leaf tissue to measure exact quantities of mRNA GFP transcripts at a given time, to quantify precise changes in the gene expression levels (see Methods). No silencing is observed in the non-treated leaf nor in leaves infiltrated with non-targeting RNA-CNTs (Fig. 4c),

as expected. Delivery of free GFP-targeting siRNA induces 30% silencing, whereby gene silencing increases to 95% when GFP-targeting siRNA is delivered via CNT scaffolding (Fig. 4c). It is not uncommon for siRNA molecules to internalize into the plant cells freely with low efficiency.[32] However, gene silencing is over three times stronger when siRNA is delivered via CNT scaffolding compared to free delivery of siRNA. It is likely that the CNT scaffold improves internalization of siRNA and also protects siRNA from degradation. 7-days following the introduction of siRNA-CNTs, GFP expression returns to baseline levels as observed in non-treated leaves, demonstrating that CNT-mediated gene silencing is transient in plants (Fig. 4d).

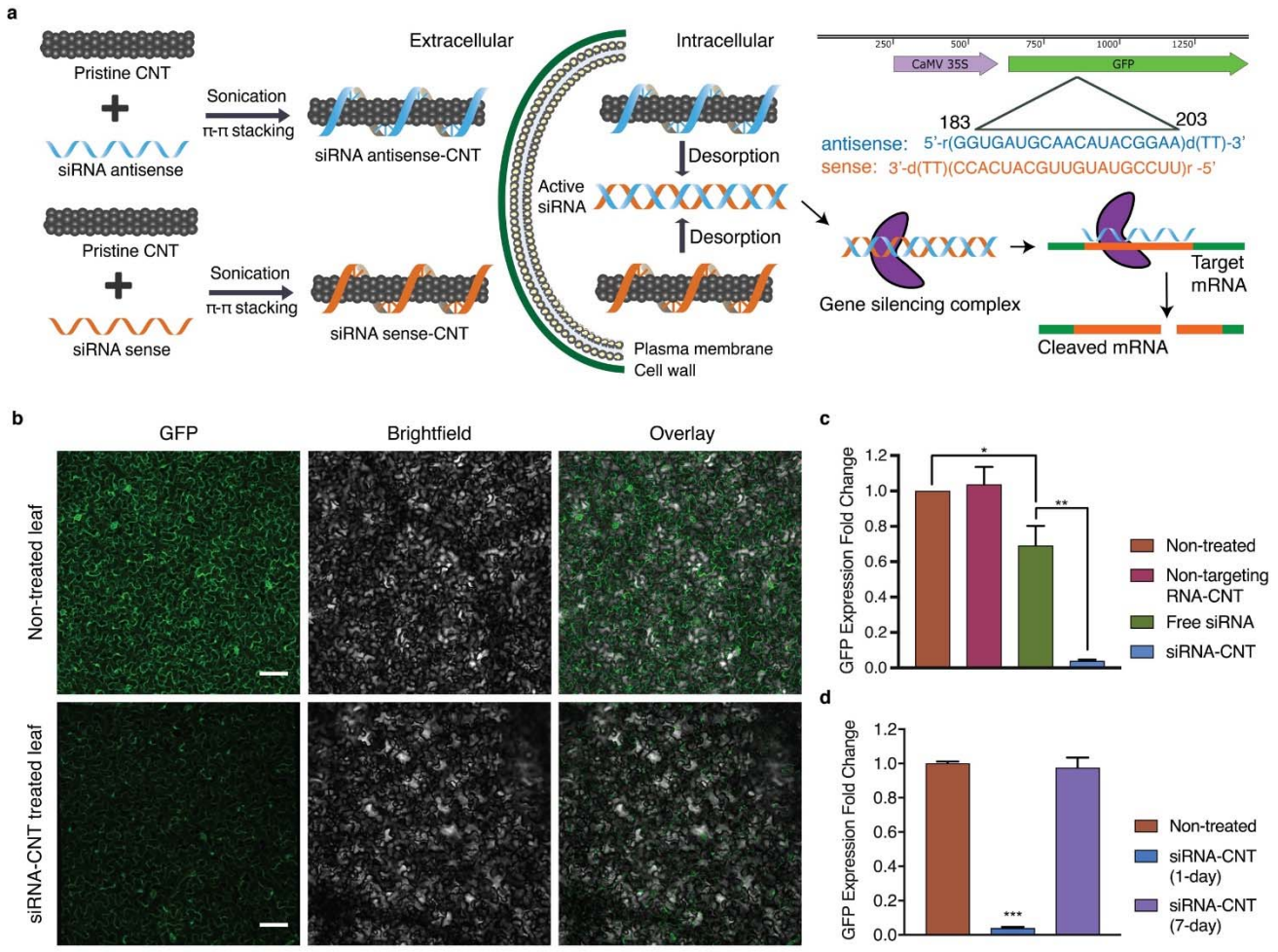

Figure 4. CNT-guided siRNA gene silencing in mature plants. a, Loading of siRNA on CNTs is accomplished by separately grafting siRNA sense and antisense sequences on CNTs via probe-tip sonication of each single-strand of the siRNA duplex. Post-infiltration, RNA-CNTs traverse the plant cell wall and membrane, and reach the cytosol. The complementary siRNA strands hybridize to each other and desorb from the CNT surface to form active double stranded siRNA. The siRNA activates the gene silencing complex, and acts as a template for complementary mRNA transcript recognition and cleavage, resulting in gene silencing. **b**, Untreated leaves show strong GFP expression due to constitutive expression of GFP in the transgenic plant, whereas leaves infiltrated with siRNA-CNTs show strongly reduced GFP fluorescence, suggesting effective siRNA-CNT mediated gene silencing. Scale bars, 100 μm. **c**, Quantitative PCR (qPCR) results show no gene silencing in the non-treated leaf nor in leaves infiltrated with non-targeting RNA-CNTs. Delivery of free GFP-targeting siRNA induces 30% silencing, whereby

gene silencing increases to 95% when GFP-targeting siRNA is delivered via CNT scaffolding. Two-tailed P value for * is 0.0498 and for ** is 0.0042. Error bars are standard errors of the mean (n = 3). **d**, GFP expression nearly returns to its initial value 7 days post-infiltration with siRNA-CNT, suggesting transient gene silencing with CNT nanocarriers. Two-tailed P value for *** is smaller than 0.0001. Error bars are standard errors of the mean (n = 3).

qPCR analysis, through normalization with the plant reference gene elongation factor 1 (EF1) expression[33], confirms that the observed decrease in GFP expression is triggered by CNT-mediated siRNA delivery, and not due to infiltration-mediated damage of the leaf tissue. Furthermore, we have performed toxicity analyses to confirm that the decrease in GFP expression trigged by CNT-mediated siRNA gene silencing is not due to damaged or unhealthy plant leaf tissue. Specifically, we performed qPCR analysis of respiratory burst oxidase homolog B (NbrbohB) upregulation, a known stress gene in *benthamiana* plants.[34] Quantification of NbrbohB expression shows that CNT-treated areas in leaves do not upregulate NbrbohB compared to adjacent areas within the same leaves treated only with buffer (0.1 M NaCl). Additionally, quantum yield measurements of photosystem II[35] show that CNT-infiltrated areas in the *benthamiana* plant leaf have similar photosynthesis quantum yields as control areas within the same leaves without CNT infiltration (see Methods). Positive controls to induce plant stress for both NbrbohB qPCR and photosystem II quantum yield measurements show clear upregulation of NbrbohB and significant decrease in photosystem II quantum yield in *benthamiana* (Supplementary Fig. 9.). Our analysis suggests our CNT-based platform for RNA delivery is effective for siRNA-mediated gene silencing in mature plants, without inducing toxicity.

Conclusions and potential of CNT-mediated delivery in plants

Genetic engineering of plants may address the crucial challenge of cultivating sufficient food and natural product therapeutics for an increasing global population living under changing climatic conditions. Despite advances in genetic engineering across many biological species, the transport of genetic material into plant cells and nuclei remain the primary limitation for broad-scale implementation and high-throughput testing of genetic engineering tools, particularly for mature plants with walled cells. Additionally, regulatory oversight for genetically-modified foods (GMOs) motivate the development of plant engineering technologies for which gene expression is transient and foreign DNA is not integrated into the host plant genome. We have developed a CNT-based delivery tool that can transfer functional DNA and RNA biomolecules into both model

and crop plants with high efficiency and without transgenic DNA integration, as shown by two proof-of-concept examples of gene expression and silencing.

The nanomaterial-based transient plant transformation technology we have developed herein is beneficial for plant biotechnology applications where gene expression without transgene integration is desired, and where multiple genes are to be tested rapidly and in parallel.[36] This technology may aid high-throughput screening of mature plants to rapidly identify genotypes that result in desired phenotypes, mapping and optimization of plant biosynthetic pathways, and maximization of plant-mediated natural product synthesis, most of which currently rely on agrobacterial transformation.[37] CNT-mediated DNA and RNA delivery to plants is easier and faster than agrobacterium-mediated plant transformation, amenable to multiplexing, and scalable, enabling its broad-scale adoption. Our CNT nanomaterial-mediated delivery platform may enable high-throughput transient plant transformations, which have numerous impactful applications such as the synthesis of novel small-molecule drugs and recombinant proteins in plant cells, engineering plants for more efficient and cleaner biofuels, and creating crops that are resistant to drought, insects, herbicides, and disease. These overarching goals form the core arsenal of our sustainability efforts, both at the levels of food availability and environmental remediation.

Acknowledgments

We acknowledge support of a Burroughs Wellcome Fund Career Award at the Scientific Interface (CASI), the Simons Foundation, a Stanley Fahn PDF Junior Faculty Grant with Award # PF-JFA-1760, a Beckman Foundation Young Investigator Award, and a FFAR New Innovator Award. M.P.L. is a Chan Zuckerberg Biohub investigator. G.S.D. is supported by a Schlumberger Foundation Faculty for the Future Fellowship. L.C. is supported by National Defense Science and Engineering Graduate (NDSEG) Fellowship and by the LAM Foundation. The authors wish to thank Alex Schultink, Arturo Ortega, Dr. Juliana De Lima Matos, and Dr. Brian Staskawicz for helpful discussions, and Dr. Christopher Jakobson and Dr. Danielle Tullman-Ercek for generously sharing their lab resources. We acknowledge the support of the UC Berkeley Molecular Imaging Center, the QB3 Shared Stem Cell Facility, and the IGI.

Author contributions

G.S.D. and M.P.L. conceived of the project, designed the study, and wrote the paper. G.S.D. and R.C. performed experiments and data analysis. H.Z. and L.C. performed AFM imaging and

data analysis. All authors have commented on the manuscript and have given their approval of the final version.

Competing financial interests

The authors declare no competing financial interests.

References

1. Daniell, H., Datta, R., Varma, S., Gray, S. & Lee, S.-B. Containment of herbicide resistance through genetic engineering of the chloroplast genome. *Nat Biotech* **16**, 345-348 (1998).
2. Liu, Y. *et al.* A gene cluster encoding lectin receptor kinases confers broad-spectrum and durable insect resistance in rice. *Nat Biotech* **33**, 301-305, doi:10.1038/nbt.3069 (2015).
3. Li, T., Liu, B., Spalding, M. H., Weeks, D. P. & Yang, B. High-efficiency TALEN-based gene editing produces disease-resistant rice. *Nat Biotech* **30**, 390-392, doi:10.1038/nbt.2199 (2012).
4. Zhang, G. *et al.* Overexpression of the soybean GmERF3 gene, an AP2/ERF type transcription factor for increased tolerances to salt, drought, and diseases in transgenic tobacco. *Journal of Experimental Botany* **60**, 3781-3796, doi:10.1093/jxb/erp214 (2009).
5. Chen, Q. & Lai, H. Gene delivery into plant cells for recombinant protein production. *Biomed Res Int* **2015**, 932161, doi:10.1155/2015/932161 (2015).
6. Himmel, M. E. *et al.* Biomass Recalcitrance: Engineering Plants and Enzymes for Biofuels Production. *Science* **315**, 804 (2007).
7. Tufekcioglu, A., Raich, J., Isenhart, T. & Schultz, R. Biomass, carbon and nitrogen dynamics of multi-species riparian buffers within an agricultural watershed in Iowa, USA. *Agroforestry Systems* **57**, 187-198 (2003).
8. Altpeter, F. *et al.* Advancing Crop Transformation in the Era of Genome Editing. *Plant Cell* **28**, 1510-1520, doi:10.1105/tpc.16.00196 (2016).
9. Herrera-Estrella, L., Depicker, A., Van Montagu, M. & Schell, J. Expression of chimaeric genes transferred into plant cells using a Ti-plasmid-derived vector. *Nature* **303**, 209-213 (1983).
10. Baltes, N. J., Gil-Humanes, J. & Voytas, D. F. Genome Engineering and Agriculture: Opportunities and Challenges. *Progress in Molecular Biology and Translational Science* (2017).
11. Klein, T. M., Wolf, E., Wu, R. & Sanford, J. High-velocity microprojectiles for delivering nucleic acids into living cells. *Nature* **327**, 70-73 (1987).
12. Russell, J. A., Roy, M. K. & Sanford, J. C. Physical trauma and tungsten toxicity reduce the efficiency of biolistic transformation. *Plant Physiology* **98**, 1050-1056 (1992).
13. Song, S., Hao, Y., Yang, X., Patra, P. & Chen, J. Using gold nanoparticles as delivery vehicles for targeted delivery of chemotherapy drug fludarabine phosphate to treat hematological cancers. *Journal of nanoscience and nanotechnology* **16**, 2582-2586 (2016).
14. Mizrachi, A. *et al.* Tumour-specific PI3K inhibition via nanoparticle-targeted delivery in head and neck squamous cell carcinoma. *Nature Communications* **8**, 14292 (2017).
15. Demirer, G. S. & Landry, M. P. Delivering Genes to Plants. *CHEMICAL ENGINEERING PROGRESS* **113**, 40-45 (2017).
16. Wong, M. H. *et al.* Lipid exchange envelope penetration (LEEP) of nanoparticles for plant engineering: A universal localization mechanism. *Nano letters* **16**, 1161-1172 (2016).
17. Giraldo, J. P. *et al.* Plant nanobionics approach to augment photosynthesis and biochemical sensing. *Nature materials* **13**, 400-408 (2014).
18. Wu, Y., Phillips, J. A., Liu, H., Yang, R. & Tan, W. Carbon nanotubes protect DNA strands during cellular delivery. *ACS nano* **2**, 2023-2028 (2008).
19. Zheng, M. *et al.* DNA-assisted dispersion and separation of carbon nanotubes. *Nature materials* **2**, 338 (2003).

20. Wang, H. *et al.* High-yield sorting of small-diameter carbon nanotubes for solar cells and transistors. *ACS nano* **8**, 2609-2617 (2014).
21. Liu, Q. *et al.* Carbon nanotubes as molecular transporters for walled plant cells. *Nano letters* **9**, 1007-1010 (2009).
22. Serag, M. F. *et al.* Trafficking and subcellular localization of multiwalled carbon nanotubes in plant cells. *ACS nano* **5**, 493-499 (2010).
23. Wong, M. H. *et al.* Nitroaromatic detection and infrared communication from wild-type plants using plant nanobionics. *Nature materials* **16**, 264-272 (2017).
24. Choi, J. H. & Strano, M. S. Solvatochromism in single-walled carbon nanotubes. *Applied Physics Letters* **90**, 223114 (2007).
25. Alidori, S. *et al.* Deploying RNA and DNA with functionalized carbon nanotubes. *The Journal of Physical Chemistry C* **117**, 5982-5992 (2013).
26. Boehr, D. D., Farley, A. R., Wright, G. D. & Cox, J. R. Analysis of the π-π stacking interactions between the aminoglycoside antibiotic kinase APH (3′)-IIIa and its nucleotide ligands. *Chemistry & biology* **9**, 1209-1217 (2002).
27. Schaumberg, K. A. *et al.* Quantitative characterization of genetic parts and circuits for plant synthetic biology. *Nature methods* **13**, 94 (2016).
28. Yoo, S.-D., Cho, Y.-H. & Sheen, J. Arabidopsis mesophyll protoplasts: a versatile cell system for transient gene expression analysis. *Nature protocols* **2**, 1565 (2007).
29. Hannon, G. J. RNA interference. *Nature* **418**, 244-251 (2002).
30. Wittrup, A. & Lieberman, J. Knocking down disease: a progress report on siRNA therapeutics. *Nature reviews. Genetics* **16**, 543 (2015).
31. Tang, W. *et al.* Post-transcriptional gene silencing induced by short interfering RNAs in cultured transgenic plant cells. *Genomics, proteomics & bioinformatics* **2**, 97-108 (2004).
32. Mitter, N. *et al.* Clay nanosheets for topical delivery of RNAi for sustained protection against plant viruses. *Nature plants* **3**, 16207-16207 (2017).
33. Schmidt, G. W. & Delaney, S. K. Stable internal reference genes for normalization of real-time RT-PCR in tobacco (Nicotiana tabacum) during development and abiotic stress. *Molecular Genetics and Genomics* **283**, 233-241, doi:10.1007/s00438-010-0511-1 (2010).
34. Yoshioka, H. *et al.* Nicotiana benthamiana gp91phox homologs NbrbohA and NbrbohB participate in H2O2 accumulation and resistance to Phytophthora infestans. *The Plant Cell* **15**, 706-718 (2003).
35. Van Kooten, O. & Snel, J. F. The use of chlorophyll fluorescence nomenclature in plant stress physiology. *Photosynthesis research* **25**, 147-150 (1990).
36. Sullivan, A. M. *et al.* Mapping and dynamics of regulatory DNA and transcription factor networks in A. thaliana. *Cell reports* **8**, 2015-2030 (2014).
37. Lau, W. & Sattely, E. S. Six enzymes from mayapple that complete the biosynthetic pathway to the etoposide aglycone. *Science* **349**, 1224-1228 (2015).

Methods

Procurement and preparation of chemicals and nanomaterials. Super purified HiPCO SWCNTs (Lot # HS28-037) were purchased from NanoIntegris, MWCNTs (Lot # R0112) were purchased from NanoLab, and both CNT samples were extensively purified[1] before use. Carboxylic acid functionalized SWCNTs (Lot # MKBX0303V) and MWCNTs (Lot # BCBR9248V) were purchased from Sigma-Aldrich. GFP-encoding plasmids (35S-GFP-NOS and UBQ10-GFP-NOS) were obtained from the Sheen Lab, Harvard Medical School[2]. 20K MWCO dialysis cassettes were purchased from Thermo Scientific. The following chemicals were purchased from Sigma-Aldrich: sodium dodecyl sulfate (molecular biology grade), sodium chloride, MES hydrate, D-mannitol, calcium chloride dihydrate (suitable for plant cell culture), potassium chloride, magnesium chloride hexahydrate, bovine serum albumin (heat shock fraction), polyethylene glycol (4K), and polyethylenimine (branched, 25K). Cellulase R10 and macerozyme R10 enzymes were purchased from Grainger. Single stranded RNA and DNA polymers were purchased from IDT and dissolved in 0.1M NaCl before use. UltraPure DNase/RNase-free distilled water from Invitrogen was used for qPCR experiments, and EMD Millipore Milli-Q water was used for all other experiments.

Plant growth. Italian arugula *(Eruca sativa)* seeds purchased from Renee's Garden were germinated in SunGro Sunshine LC1 Grower soil mix by planting the seeds half an inch deep into the soil of a standard propagation liner tray (Nursery Supplies). The germinated plants were then moved to a Hydrofarm LED growth chamber (12h light at ~22˚C / 12h dark at 18˚C). Plants were allowed to mature to 3-4 weeks of age within the chamber before experimental use. Transgenic mGFP5 *Nicotiana benthamiana* seeds obtained from the Staskawicz Lab, UC Berkeley, were germinated and grown in SunGro Sunshine LC1 Grower soil mix for four weeks before experimental use.

SDS-CNT, siRNA-CNT, and ssDNA-CNT preparation. 1 mg/mL HiPCO SWCNTs were added to 3 mL 2 wt% SDS in water and bath sonicated for 10 min, followed by probe-tip sonication with a 6-mm sonicator tip at 40% amplitude (~12W) for 1h in an ice bath. The resulting solution rested at room temperature for 30 minutes before centrifugation at 16,100g for 1 h to remove unsuspended SWCNT aggregates and metal catalyst precursor. The concentration of SDS-SWCNTs was measured by recording the SWCNT absorption spectrum with a UV-Vis-nIR spectrometer and calculating the SWCNT concentration in mg/liter (absorbance at 632 nm/extinction coefficient of 0.036). The same suspension protocol applies for MWCNTs, but, their concentration was measured using a standard curve as obtained by Yang *et al.* [3].

The sequences of siRNA that were utilized for siRNA gene silencing experiments are as follows:
Sense: 5'-r(GGUGAUGCAACAUACGGAA)d(TT)-3'
Antisense: 5'-r(UUCCGUAUGUUGCAUCACC)d(TT)-3'

Sequences of the non-targeting RNA strands are:
Sense: 5'-r(UAAGGCUAUGAAGAGAUAC)d(TT)-3'
Antisense: 5'-r(GUAUCUCUUCAUAGCCUUA)d(TT)-3'

siRNA and non-targeting RNA were loaded on SWCNTs as single-stranded polymers through probe-tip sonication as previously described[4]. Briefly, the sense strand of siRNA was dissolved at a concentration of 100 mg/mL in 0.1 M NaCl. 20 µL of this RNA solution was aliquoted into 980 µL 0.1 M NaCl and 1 mg HiPCO SWCNTs

was added. The mixture was bath sonicated for 10 min, followed by probe-tip sonication with a 3-mm tip at 50% amplitude (~7W) for 30 min in an ice bath. The resulting solution rested at room temperature for 30 minutes before centrifugation at 16,100g for 1 h to remove unsuspended SWCNT aggregates and metal catalyst precursor. The same protocol was followed for the antisense strand of siRNA and non-targeting RNA strands. Unbound (free) RNA was removed via spin-filtering (Amicon, 100K) and the concentration of RNA-SWCNTs was determined by measuring the SWCNT absorbance at 632 nm. For toxicity assays, SWCNTs were suspended in single-stranded DNA (ssDNA) polymers with sequence $(AT)_{15}$. Preparation of ssDNA-SWCNTs followed the same protocol as for RNA-loaded SWCNTs, described above.

Linear DNA vector preparation from plasmid DNA. The promoter, GFP gene, and terminator regions of the 35S-GFP-NOS plasmid (obtained from the Sheen Lab, Harvard Medical School) were amplified with PCR over 35 cycles, with the following modified M13 forward and M13 reverse primers: 5'-GTAAAACGACGGCCAGT-3' and 5'-AGCGGATAACAATTTCACACAGG-3', respectively. Following PCR, pure DNA vector was obtained by using a PureLink PCR purification kit (Invitrogen) to eliminate primers, unreacted nucleotides, and enzymes. To check the amplification quality, the resulting amplicon was sent for Sanger sequencing, and was also run with agarose gel electrophoresis (see Supplementary Fig. 10 for plasmid maps and linearization results).

Direct adsorption of DNA onto CNTs via dialysis. An SDS-CNT solution containing 1 μg of CNTs, and 10 μg of free plasmid DNA were placed into an accurately-pore-sized dialysis cartridge (20K, 0.5mL), that allowed the exit of SDS monomers that desorbed from the CNT surface, while free plasmid DNA suspended the CNTs which remained inside the dialysis cartridge. If necessary due to volume considerations, 2wt% SDS was used to fill the additional volume of dialysis cartridge to ensure there was no free air space in the cartridge. After 4 days of dialysis with continuous stirring and changing the dialysis buffer (0.1M NaCl) daily, we obtained a stable suspension of plasmid DNA conjugated CNTs. A control cartridge containing 1 μg of CNTs in 2% SDS, but lacking plasmid DNA, was dialyzed in parallel to ensure that CNTs did not suspend in solution in the absence of plasmid DNA, confirming plasmid DNA adsorption to CNTs in the main sample. For results, see Supplementary Figure 1. The preparation protocol was same for both plasmids, linearized DNA vectors, and for both types of CNTs (SW- and MWCNTs).

Electrostatic grafting of DNA onto CNTs. Chemical modification of CNTs to carry positive charge is described elsewhere[5] and applied here with some modifications. A mixture of 100 mg of carboxylated CNTs suspended in water (1mg/mL) and 1 g of PEI solution was bath sonicated for several minutes, and subsequently heated at 82 °C with stirring for 16 h (the reaction can be scaled up or down as desired by keeping the PEI to CNT mass ratio constant). The reaction mixture was subsequently cooled to room temperature and filtered with a 0.4 μm and 1 μm Whatman Nucleopore membrane to filter SWCNTs and MWCNTs, respectively. The filtered product was washed vigorously with water 5 times to remove unreacted PEI from the reaction mixture, then dried and collected. 3 mg of dried product (PEI-CNT) was subsequently suspended in 3 mL water by probe-tip sonication with a 6-mm tip at 40% amplitude (~12W) for 1h in an ice bath. The resulting solution was rested at room temperature for 30 minutes before centrifugation at 16,100g for 1 h to remove unsuspended CNT aggregates. The PEI-CNT solution containing 1 μg of CNTs was added into 0.2 μg of DNA dropwise, pipetted in and out 10 times, and incubated at room

temperature for 30 min so that negatively charged DNA adsorbed on PEI-CNTs (DNA incubation can be scaled up or down as well by keeping the DNA to PEI-CNT mass ratio constant).

Infiltration of leaves with CNTs. Healthy and fully-developed leaves from *Eruca sativa* (arugula) plants (3-4 weeks old) and *Nicotiana benthamiana* plants (4 weeks old) were selected for experiments. A small puncture on the abaxial surface of the *Eruca sativa* leaf lamina was introduced with a pipette tip, and 100 µL of the plasmid DNA-CNT solution was infiltrated from the hole with a 1 mL needleless syringe by applying a gentle pressure, with caution not to damage the leaf. For *Nicotiana benthamiana* infiltration, a tiny puncture on the abaxial surface of the leaf lamina was introduced with a sharp razor, and 100 µL of siRNA-CNT solution was infiltrated through the puncture with a 1 mL needleless syringe by applying a gentle pressure. After infiltration, leaves were left in the plant growth chamber (for arugula) and in plant pots (for *benthamiana*) to allow for gene expression and silencing, and imaged after 72 and 24 h, respectively, prior to quantifying gene expression and silencing.

Quantitative fluorescence intensity analysis of GFP gene expression. Infiltrated *Eruca sativa* plant leaves were prepared for confocal imaging 72 hours post-infiltration with DNA-CNT by cutting a small leaf section of the infiltrated leaf tissue, and inserting the tissue section between a glass slide and cover slip of #1 thickness. 100 µL water was added between the glass slide and cover slip to keep the leaves hydrated during imaging. A Zeiss LSM 710 confocal microscope was used to image the plant tissue with 488 nm laser excitation and with a GFP filter cube. GFP gene expression images were obtained at 10x magnification. Confocal image data was analyzed to quantify GFP expression across samples. For each sample, 3 biological replicates (3 infiltrations into 3 different plants) were performed, and for each biological replicate, 15 technical replicates (15 non-overlapping confocal field of views from each leaf) were collected. Each field of view was analyzed with custom ImageJ analysis to quantify the GFP fluorescence intensity value for that field of view, and all 15 field of views were then averaged to obtain a mean fluorescence intensity value for that sample. The same protocol was repeated for all 3 biological replicates per sample, and averaged again for a final fluorescence intensity value, which correlates with the GFP expression produced by that sample. Analysis was conducted in the same way for all samples, statistical significance between samples was determined with a t-test, and standard errors were plotted on graphs as error bars (with n=3 biological replicates).

Protoplast isolation from *Eruca sativa* leaves. Protoplasts were isolated from arugula leaves as described by Yoo *et al.*[2] with some modifications. Briefly, thinly cut arugula leaf strips were immersed in 20 mL of enzyme solution (consisting of cellulase and macerozyme), vacuum infiltrated for an hour in the dark using a desiccator, and further incubated at 37˚C for 3 hours in the dark without stirring. Undigested leaf tissue was removed by filtration with a 75 µm nylon mesh, and the flow-through was centrifuged at 200 g for 3 min to pellet the protoplasts in a round bottom tube. Pelleted protoplasts were resuspended in 0.4 M mannitol solution (containing 15 mM $MgCl_2$ and 4 mM MES) with a pH of 5.7, which has similar osmolarity and pH to the protoplasts. Isolated protoplasts can be kept viable on ice for over 24 h; however, we used only freshly isolated protoplasts for all gene expression studies.

Protoplast transformation with DNA-CNTs. 100 µL (~2x10^4) of isolated protoplasts in mannitol solution were added to 10 µg CNT-plasmid DNA (250ng/µL DNA concentration), or for the control sample only plasmid DNA (250ng/µL DNA concentration) and mixed well by gently tapping the tube. The mixture was incubated at room temperature for 1 h, and subsequently centrifuged at 200g for 3 min to pellet protoplasts. Protoplasts were resuspended in 1 mL of 0.5 M mannitol solution (containing 4mM MES and 20 mM KCl at pH 5.7) in a non-culture treated 6 well-plate (Corning) for 24 hours in the dark. Protoplasts settled to the bottom of the well plate. Fluorescence microscopy was performed through the well-plate to image the protoplast cells and to measure GFP expression for quantification of transformation efficiency.

Quantitative PCR (qPCR) experiments and data analysis. Two-step qPCR was performed to quantify GFP gene silencing in transgenic *Nicotiana benthamiana* plants with the following commercially-available kits: RNeasy plant mini kit (QIAGEN) for total RNA extraction from leaves, iScript cDNA synthesis kit (Bio-Rad) to reverse transcribe total RNA into cDNA, and PowerUp SYBR green master mix (Applied Biosystems) for qPCR. The target gene in our qPCR was mGFP5 (GFP transgene inserted into *Nicotiana benthamiana*), and EF1 (elongation factor 1) as our housekeeping (reference) gene. Primers for these genes were ordered from IDT. For mGFP5, primers used are:
Sense: 5'- AGTGGAGAGGGTGAAGGTGATG-3'
Antisense: 5'- GCATTGAACACCATAAGAGAAAGTAGTG-3'.

Primers for EF1 are:
Sense: 5'-TGGTGTCCTCAAGCCTGGTATGGTTGT-3'
Antisense: 5'- ACGCTTGAGATCCTTAACCGCAACATTCTT-3'.

An annealing temperature of 60˚C was used for qPCR, which we ran for 40 cycles.

qPCR data was analyzed by the ddCt method[6] to obtain the normalized GFP gene expression-fold change with respect to the EF1 housekeeping gene and control sample. For each sample, qPCR was performed as 3 technical replicates (3 reactions from the same isolated RNA batch), and the entire experiment consisting of independent infiltrations and RNA extractions from different plants was repeated 3 times (3 biological replicates). Statistical significance between samples was determined with a t-test, and standard errors were plotted on graphs as error bars (with n=3 biological replicates).

Plant toxicity analysis. To test for plant stress and toxicity, the expression level of an oxidative stress gene (NbRbohB)[7] in *Nicotiana benthamiana* leaves was measured through qPCR with the following primers:
Sense: 5'-TTTCTCTGAGGTTTGCCAGCCACCACCTAA-3'
Antisense: 5'-GCCTTCATGTTGTTGACAATGTCTTTAACA-3'.

EF1 was again measured as a housekeeping gene with the same primer set as described above. An annealing temperature of 60˚C was used for qPCR, which we ran for 40 cycles, and the ddCt method was used to obtain the normalized NbRbohB expression-fold change with respect to the EF1 housekeeping gene and control sample. For each sample, 3 technical and 3 biological replicates were performed. Statistical significance between samples was

determined with a t-test, and standard errors were plotted on graphs as error bars (with n=3 biological replicates). For results, see Supplementary Figure 9.

As an additional toxicity assay, Fv/Fm ratios[8] of infiltrated *Nicotiana benthamiana* leaves were measured with an Imaging-PAM Maxi fluorimeter (Walz). A singular leaf was infiltrated from the abaxial surface, in three distinct locations within the same leaf, with buffer (0.1 M NaCl), 1 mg/L DNA-CNTs, or 10% SDS (positive control for toxicity). The fourth quadrant of the leaf was left unperturbed. The triply-infiltrated leaf was subsequently incubated for 24 hours without further perturbation. Subsequently, the infiltrated leaf was dark-adapted for 15-30 minutes and chlorophyll fluorescence-related parameters were measured with the Imaging-PAM Maxi fluorimeter to calculate the Fv/Fm ratio, commonly used to test for plant stress. For each sample, 3 biological replicates were performed. Statistical significance between samples was determined with a t-test, and standard errors were plotted on graphs as error bars (with n=3 biological replicates). For results, see Supplementary Figure 9.

Method References

1. Del Bonis-O'Donnell, J. T. *et al.* Engineering Molecular Recognition with Bio-mimetic Polymers on Single Walled Carbon Nanotubes. *JoVE (Journal of Visualized Experiments)*, e55030-e55030 (2017).
2. Yoo, S.-D., Cho, Y.-H. & Sheen, J. Arabidopsis mesophyll protoplasts: a versatile cell system for transient gene expression analysis. *Nature protocols* **2**, 1565 (2007).
3. Yang, M., Gao, Y., Li, H. & Adronov, A. Functionalization of multiwalled carbon nanotubes with polyamide 6 by anionic ring-opening polymerization. *Carbon* **45**, 2327-2333 (2007).
4. Beyene, A. G., Demirer, G. S. & Landry, M. P. Nanoparticle□Templated Molecular Recognition Platforms for Detection of Biological Analytes. *Current protocols in chemical biology*, 197-223 (2016).
5. Ma, L. *et al.* Enhanced Li–S batteries using amine-functionalized carbon nanotubes in the cathode. *ACS nano* **10**, 1050-1059 (2015).
6. Schmittgen, T. D. & Livak, K. J. Analyzing real-time PCR data by the comparative CT method. *Nature protocols* **3**, 1101 (2008).
7. Yoshioka, H. *et al.* Nicotiana benthamiana gp91phox homologs NbrbohA and NbrbohB participate in H2O2 accumulation and resistance to Phytophthora infestans. *The Plant Cell* **15**, 706-718 (2003).
8. Van Kooten, O. & Snel, J. F. The use of chlorophyll fluorescence nomenclature in plant stress physiology. *Photosynthesis research* **25**, 147-150 (1990).